# USING HYDROGEOCHEMICAL APPROACH IN GROUNDWATER INVESTIGATION OF EL HEIZ AREA, EL BAHARIYA OASIS, WESTERN DESERT, EGYPT

**Gomaa, Mohamad A., Jilan A. Omar, Hesham A. Ezzeldin*, Yousra H. Kotp and Saad A. Mohallel**
Department of Hydrogeochemistry, Desert Research Center, Cairo, Egypt
*E-mail: h.ezzeldin@drc.gov.eg; h.ezzeldin@hotmail.com

El Heiz area, a part of El-Bahariya Oasis, is distinguished by nonrenewable Nubian Sandstone Aquifer System (NSAS) that has a large amount of fresh water. 16 groundwater samples were collected from multilayered Nubian Sandstone Aquifer (NSA) for physical, chemical and isotopic analysis. The average values of the total dissolved solids (TDS) indicated fresh water types with values that ranged between 149 mg/l and 544 mg/l with an average of 257 mg/l. However, the measured pH values showed relatively acidic water with values that ranged from 5.77 to 6.74 and averaged on 6.3. The measured temperature degrees varied greatly with values ranged from 26.3ºC to 46.4ºC. The stable isotopic content is also variable, where it ranged from -9.84 to -2.28 (on average -6.0) and from -79.90 to -48.63 (on average -62.20) for $\delta^{18}O$ and D, respectively. The wide range in stable isotope values indicates variable geochemical processes. The results of some trace elements such as iron and manganese showed values that exceeded the permissible limit for drinking purposes in some of the studied groundwater samples. PHREEQC program was applied to calculate the saturation indices of some selected minerals such as anhydrite, gypsum halite, calcite, dolomite, siderite and hematite to identify the role of the geochemical process on groundwater evolution. The factor analysis suggested three factors that impacted groundwater quality, including the evaporation and/or geothermal, rock–water interaction, and ion exchange processes. In general, the application of the aforementioned methods showed that the groundwater extracted from the Nubian Sandstone Aquifer (NSA) is primarily recharged from the paleo-water, which was subjected to evaporation, geothermal, leaching, and dissolution processes.

**Keywords:** groundwater, chemistry, stable isotopes, Nubian sandstone

## INTRODUCTION

Egypt relies on groundwater sources as one of the means to compensate for the water shortage. The Nubian sandstone aquifer (NSA) is one of the most important of such sources. However, it is not acceptable to randomly exploit groundwater without taking into account the means that would rationalize water consumption in a way that ensures its sustainability (Foster and Loucks, 2006).

Due to its substantial economic resources, including as iron ore reserves, hydrocarbon-producing fields, archaeological monuments, and huge reclaimable areas, El-Bahariya Oasis is a fascinating location that has attracted attention. The most significant source of groundwater, not only in El-Bahariya Oasis but also in the Western Desert, is the Nubian sandstone aquifer (Hamdan and Sawires, 2013). The Ministry of Public Works and Water Resources (1998) reported that the shallow and natural springs were the sole water sources accessible for domestic and agricultural usage in the El-Bahariya Oasis before the 60$^{th}$ of the past century. Afterwards, deep well drilling was started because of growing population and farmed regions. The excessive and random drilling of wells along with the overexploitation of groundwater led to a continuous lowering of the groundwater level (Abd El-Latif, 2007). Many deep artesian wells have now become pumped wells, rather than shallow naturally flowing wells, because of intensive groundwater extraction from the Nubian Sandstone Aquifer. The consequences of such practices along with other factors including urbanization, population growth, land reclamation, a rise in agricultural operations, and improper irrigation and drainage systems lead to groundwater quality and quantity deterioration (Khazaei et al., 2004 and Polemio et al., 2009). Additionally, the geological and hydrological features of the region, which determine the time and directions of flow and the water quality, have an impact on groundwater (Prior et al.,, 2003). El-Heiz area located at the southern part of El-Bahariya Oasis was selected as a pilot location to study the hydrogechemical characteristics of groundwater. Groundwater in El-Bahariya is extracted from the NSA, which is divided into three zones separated by clay and shale units: the lower zone (S1), the middle zone (S2), and the upper zone (S3), (Sharaky and Abdoun, 2020).

The current study will benefit from the geologic structures and the hydrologic conditions as well as the chemical analysis data to study the groundwater characteristics in the study area. Additionally, the manuscript will shed light on the impact of rock-water interaction on the geothermal fluids. The chemistry of geothermal fluids is an important and complex topic that can explain the change in the chemical composition of the fluids because of geothermal activity. The chemical composition of geothermal fluids can differ significantly depending on the location and type of geothermal system (Karingithi, 2009). Some geothermal fluids may have

high levels of silica, while others may contain high concentrations of sulfur and other dissolved gases. Moreover, the chemical composition of geothermal fluids can change over time due to variations in temperature, pressure, and the surrounding geological environment (Su et al., 2022).

Different approaches such as: graphical representations, bivariate relationships, multivariate statistical analysis, geochemical modeling and stable isotopes will be applied. Based on the chemical datasets, such methods assist in classifying groundwater and identifying the primary factors that impacted the chemistry of the groundwater.

## 1. Study Area Location and Topography

El-Heiz area, located in the southwestern of the El-Bahariya Oasis, is bounded between latitudes 27° 48′ and 28° 30′ N and longitudes between 28° 35′ and 29° 10′ E about 400 km southwest of Cairo. Due to the erosion of hard rocks distributed in El-Bahariya Oasis, its topography is characterized by a flat, rough, rocky surface that is ranging in high between 71 and 370 meters above mean sea level (AMSL) (Fig. 1). Generally, the northern and southern sectors of Baharyia Oasis is characterized by flat surfaces, whereas the central section is rough and higher in elevation.

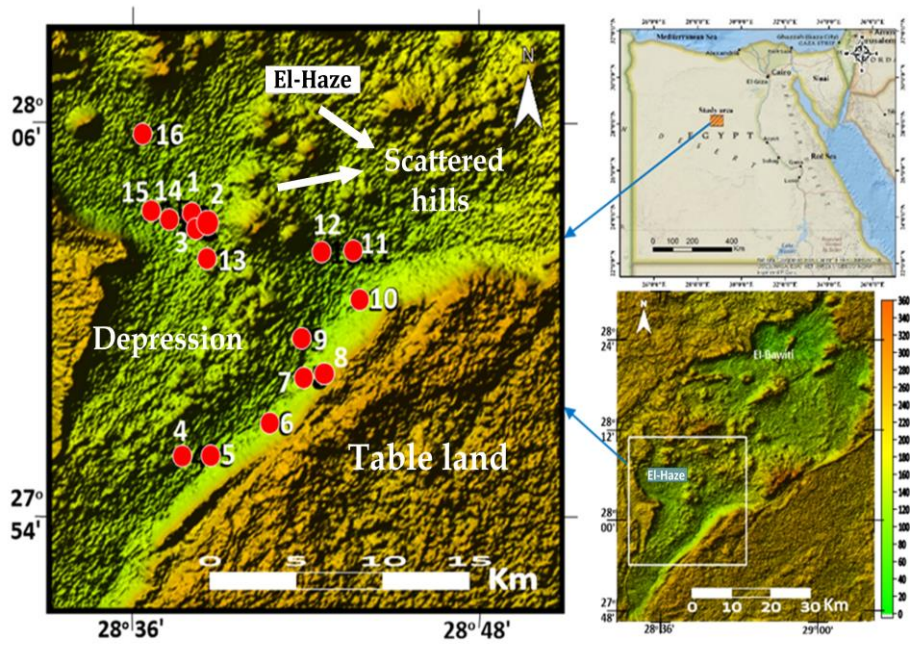


**Fig. (1).** Study area showing the geomorphologic features and wells locations.

The most remarkable geomorphic units are the plateau surface, surrounding rocky outcrops, oasis floor, plains, sedimentary deposits and terraces, igneous wedges and sheets, evaporites and sands (Embabi and El Kayali, 1979).

## 2. Geology and Hydrology

Generally, El-Baharyia Oasis is characterized by sedimentary cover of rocks that ranging from upper Cretaceous to Quaternary in age (Fig. 2). The stratigraphic sequence in El-Bahariya Oasis is briefly described from the oldest (bottom) to the youngest as follows (El Akkad and Issawi, 1963):

- Pre-Cambrian Basement Rocks; they are composed of dense, grey metamorphic rocks.
- Cambrian Rock; they are composed of intercalated siltstone, sandstone, and clay of 458 m thick.
- Cretaceous rocks; a 660-meter section lies on top of Cambrian deposits of intercalated undifferentiated sandstones, sands, and clays. From bottom to top, they are divided into four formations: El-Bahariya Formation (Lower Cenomanian), El-Heiz Formation (Upper Cenomanian), El-Hefhuf Formation (Campanian-Turonian), and Khoman Formation (Maastrichtian).
- Paleocene Rock; they are represented by Tarawan Chalk (Lower Paleocene) and Esna Shale (Upper Paleocene-Lower Eocene).
- Eocene rocks, also known as Eocene limestone rocks, form the eroded plateau surface surrounding El-Bahariya depression and some of its isolated hills. The Eocene strata rest irregularly on Upper Cretaceous rocks. Farafra Formation, Naqb Formation (Lower Middle Eocene), Qazzun Formation (Upper Middle Eocene), and El-Hamra Formation comprise it (Middle-Upper Eocene).
- Tertiary Rocks; they are composed of numerous isolated basalt outcrops of Oligocene-aged volcanic rocks distributed in the northern and central parts of the depression.
- Quaternary deposits; they are formed of aeolian sands; sabkhas and salt deposits; fine sand, silt, clay, gypsum, and halite.

According to Khalifa (2006), the groundwater-bearing horizons in El-Bahariya area from top to bottom are:

1. The Post-Nubian sandstone aquifer; it composed of marine sediments and mainly consist of clay, marl, and limestone overlain by continental clastic sediments. This sequence ranges in age from Late Cenomanian to the recent.
2. The Nubian sandstone aquifer system, which represents the main water-bearing horizon in the study area. It consists of continental clastic sediments mainly sandstone alternating with shale and clays. These series were classified stratigraphically into three units in El-Bahariya Formation, namely Cenomanian water bearing horizon (0–705 m), Pre-Cenomanian water-

bearing horizon (705–1,355 m; 650 m thick), and Cambrian water-bearing horizon (1,366–1,823 m; 460 m thick) (Diab, 1972). This aquifer is confined due to the clays and shales that overlie and underlie the sandstone layers. The underlying basement rocks from the Precambrian period form the base of this aquifer (Sharaky and Abdoun, 2020). Both the Nubian and Post-Nubian aquifers are hydraulically-connected that permit upward leakage (Abd El-Latif, 2007). A southwest-north east hydrogeological cross-section, is presented to show the Nubian Sandstone zones in El-Bahariya Oasis (Fig. 3).

In El-Heiz area, groundwater exists in El-Heiz Formation that belongs to the Cenomanian aquifer. This formation is composed of successive layers of dolomitic sandstones interbedded with shale and clay layers (Himida, 1964 and Abdel Ati, 1995). According to Sharaky and Abdoun (2020), such layers can be differentiated into three horizons; the lower sandstone zone ($S_1$), which is represented by one deep well (sample no. 13); the middle sandstone zone ($S_2$) that is penetrated by three wells (samples nos. 1, 14 and 15); and the shallower sandstone zone ($S_3$) that is tapped by the majority of the groundwater samples (11 wells).

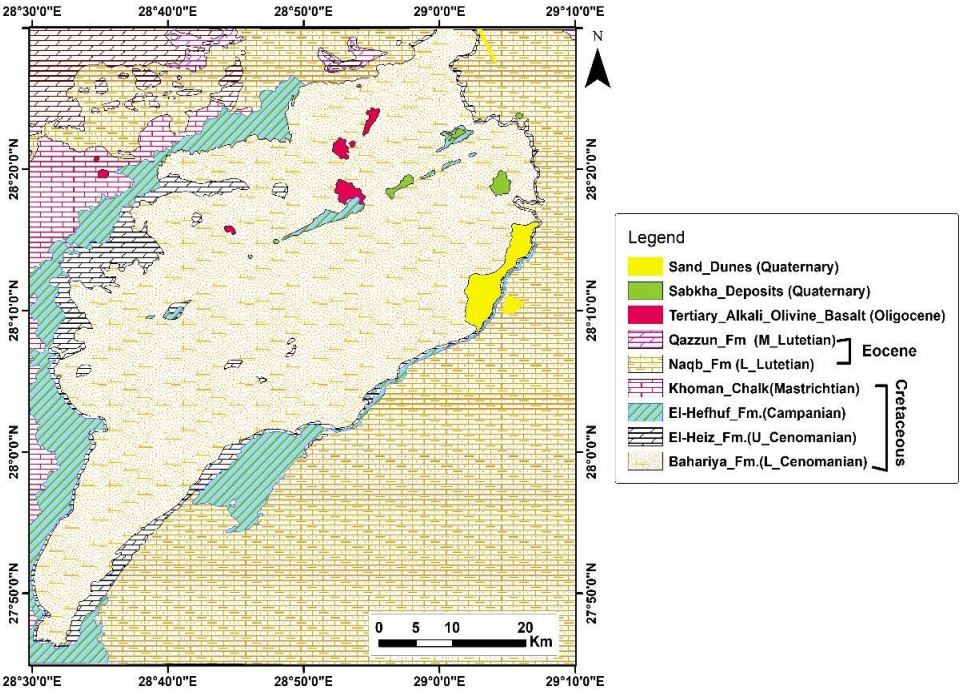


**Fig. (2).** Outcropping rocks in El-Baharyia Oasis (Conoco, 1987).

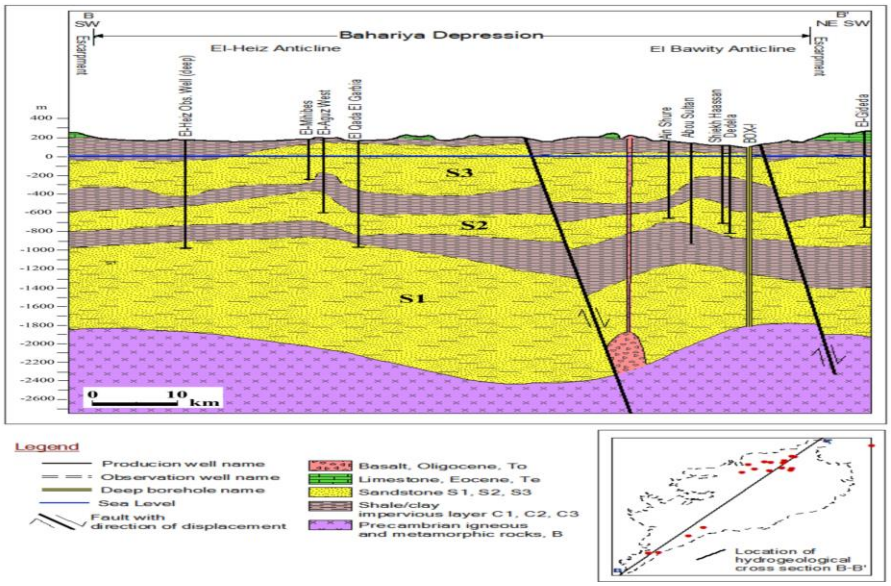


**Fig. (3).** Hydrogeological cross section in El-Bahariya Oasis showing the NSA zones S1, S2 and S3 (RIGW, 2010).

## MATERIALS AND METHODS

### 1. Sample Collection and Analysis

During January 2021, 16 groundwater samples were collected from private and governmental wells, located in El-Heiz area, for major ions, trace elements and stable isotopes determination. The precise sampling locations were determined using GPS. The temperature, pH, and conductivity (EC) of each sample were measured in the field using a portable pH and EC meter (Hanna HI8424 and GLF-100RW conductivity meter).

By using the neutralization method, carbonates ($CO_3$) and bicarbonates ($HCO_3$) were measured titrimetrically versus sulfuric acid. Ion chromatography (IC) was utilized to measure the remaining major ions including ($SO_4$, Cl, Ca, Mg, Na, and K) using a Dionex ICS-1100 Reagent-Free IC System. Plasma optical emission mass spectrometer (ICP) (POEMSIII, thermo Jarrell elemental company USA) was used to detect trace elements like Al, Si, Fe, and Mn. These chemical analyses were carried out at the hydrogeochemistry and central Laboratories of the Desert Research Center using the techniques adopted by the U.S. Geological Survey, Fishman and Friedman (1989) and American Society for Testing Materials (1999). The confirmation of the charge balance for the primary ionic components was within the acceptable range of ±5%.

Moreover, a Picarro L2130-I isotope analyzer was used for the performance of stable isotopes analysis such as (O-18 and deuterium) in the laboratory of the Desert Research Center, Egypt. Precision for an $\delta^{18}O/\delta D$ measurement with a liquid sample is guaranteed to be 0.025/0.1, and drift over a 24-hour period is guaranteed to be 0.2/0.8

## 2. Data Interpretation

The groundwater samples' chemical data was interpreted using a variety of techniques, including graphs, ion correlations, statistical analysis, and geochemical modelling. Piper plot (Piper, 1944) was used to identify the various chemical types of the studied groundwater samples, while Gibbs diagram (Gibbs, 1970) was adopted to recognize the primary processes that directly impacted groundwater chemistry, such as rock-water interaction, dilution, or evaporation.

The Na–K–Mg and Cl-$SO_4$-$HCO_3$ ternary diagrams proposed by Giggenbach (1988 and 1991) are used to categorize thermal water and to set apart multiple kinds of thermal waters, such as immature waters, which may indicate mixing processes or geological categories, steam heated waters, volcanic waters, and peripheral waters (Stober, 2013). These methods describe equilibration processes at different levels and up flow rates in a thermal reservoir (Han et al., 2010) and also allow a rough estimate of the temperature of the latest equilibrium. Additionally, several conventional geothermometers that are based on temperature-dependent chemical equilibria are used to process the results of the chemical analysis of specific chemical constituents (such as $SiO_2$, Na, K, Ca, and Mg). The temperature of the aquifer containing the deep waters can be determined using geothermometers that represent the equilibria of these temperature-dependent reactions (Pirlo, 2004).

The distribution and origin of the main groundwater types along the water flow paths could be explained by the hydrogeochemical facies techniques. Based on the period at which groundwater stayed in the subsurface and the degree of rock-water interaction, the facies also provide information on the progressive ion enrichment during that time. The facies are created by arranging the ionic ratios in decreasing order of abundance and disregarding less than 5% of the total ion concentration as insubstantial (Back, 1960 and Seaber, 1962). The successively dominance ions are used to determine the water type. This ordering system is primarily based on the meq/l percentages of the major cations and anions, which characterize the chemical composition of water. In denoting the water type, only such components are deemed that equates to more than 25% of the total meq/l (Zaporozec, 1972). Aquachem software (developed by waterloo hydrogeologic; Ontario, Canada) has lately been deployed to assess water types using ion ratios between 15 to 20%.

Hydrochemical coefficients (ion ratios) are correlations between the components of dissolved groundwater that show the stoichiometric balance of the different ions and suggest the plausible hydrochemical processes affecting the solution. These ratios are useful for determining the chemical changes that significantly affect quality of the water such as leaching, mixing and ion exchange. Additionally, the hydrochemical coefficients could be also employed for predicting water mixing or contamination. The coefficients which are of certain importance in this respect are Na/Cl, Ca/Mg, $SO_4$/Cl and Cl-Na/Cl.

The hydrochemical program PHREEQC is used to perform the mass-balance simulation, which shows chemical reactions and changes in chemical nature, such as the dissolution/precipitation of minerals and gases in the groundwater flow channel. The groundwater system's ability for minerals to dissolve or precipitate is demonstrated by the results of Saturation-Index (SI) values (Parkhurst and Appelo, 2013). The following equation would be used to calculate the saturation indices for the minerals that should exit or enter the solution: SI is equal to log (IAP/Kt), where Kt is the equilibrium solubility constant of the mineral and IAP is the ion-activity product in a diffused charged species solution. A negative value on the SI for any mineral phase means that the water is under saturated regarding that mineral and will disintegrate until equilibrium is attained, whilst a positive sign means that the water is oversaturated with respect to that mineral and the mineral will depart the solution or be precipitated.

SPSS, or Statistical Package for Social Sciences, is a statistical program that can be used to analyze any type of scientific data to determine the pattern of variation among variables or compressed data into a manageable number of components or components. The hydrochemical parameters (such as TDS, EC, pH, Ca, Mg, Na, K, $HCO_3$, $SO_4$, Cl-,... etc.) are among the variables used. As a result of the correlation between these variables, a correlation matrix is created (Gupta et al., 2013). To address the overall variation, Kaiser's criterion (with eigenvalues > 1), and considerable principal components (PCs) representing a percentage of variance > 10% were taken from the initial parameters. These PCs were given Varimax-rotation-generating Factors (FA) to reduce the influence of irrelevant variables. In addition to outlining the correlation between the variables and sample locations in their geographical distributions, which were grouped together based on similar environmental conditions, the FA provided the criteria for the most significant water quality measures (Zeng and Rasmussen, 2005). The correlation matrix's eigenvalues and factor loadings were calculated, and a scree plot was produced. The extraction factors were produced using the variances and covariances of the variables. The term "prominent variables" refers to variables with eigenvalues greater than one. Finally, the rotating mechanism decreases the loadings on the other factors while increasing the loadings on one of the extracted components for each

variable. $^{18}O/D$, a stable isotope that occurs naturally, was used to assess the origins of groundwater and identify the factors that affected its quality.

## RESULTS AND DISCUSSION

### 1. General physical and chemical characteristics of groundwater

Some of the data and field measurements, including the electrical conductivity (EC), temperature ($^oC$) and geographic positions as well as the total depth of the studied groundwater wells were compiled in Table (1). It is shown in this table that the measured groundwater temperatures indicated an increase with the depth as going from the shallower zone $S_3$ to the deeper zone ($S_1$), reflecting the impact of a geothermal water.

**Table (1).** Some of the data and field measurements for the studied groundwater wells in El-Heiz area.

| ID | Well type | Location | Zone | Latitude | Longitude | EC (µs/cm) | Temp. ($^oC$) | Total depth (m) |
|---|---|---|---|---|---|---|---|---|
| 1 | Governmental | Omm El Ezah | $S_2$ | 28.04711 | 28.63636 | 460 | 30.2 | 780 |
| 2 | Private | Omm El Ezah | $S_3$ | 28.05228 | 28.63183 | 373 | 26.7 | 140 |
| 3 | Private | Omm El Ezah | $S_3$ | 28.04578 | 28.63531 | 468 | 29.8 | 350 |
| 4 | Governmental | El Khabata | $S_3$ | 27.93044 | 28.62919 | 278 | 29.7 | 350 |
| 5 | Private | El Khabata | $S_3$ | 27.93114 | 28.64519 | 943 | 27.3 | 120 |
| 6 | Private | El Khabata | $S_3$ | 27.94722 | 28.67911 | 335.6 | 27.7 | 250 |
| 7 | Private | Rees | $S_3$ | 27.97078 | 28.69894 | 733.9 | 28.3 | 250 |
| 8 | Private | Rees | -- | 27.98950 | 28.71142 | 305 | 30.2 | -- |
| 9 | Governmental | Rees | $S_3$ | 27.99011 | 28.69750 | 291 | 29.7 | 350 |
| 10 | Private | Rees | $S_3$ | 28.01036 | 28.73094 | 306 | 28.3 | 150 |
| 11 | Governmental | Tabal Amoon | $S_3$ | 28.03483 | 28.72686 | 291.2 | 29.8 | 400 |
| 12 | Governmental | Aian Gomhaa | $S_3$ | 28.03436 | 28.70892 | 295 | 30.1 | 400 |
| 13 | Governmental | Omm El Ezah | $S_1$ | 28.03061 | 28.64261 | 275 | 46.4 | 1200 |
| 14 | Governmental | Hassab | $S_2$ | 28.05050 | 28.62058 | 312.4 | 30 | 600 |
| 15 | Governmental | Omm Kheleef | $S_2$ | 28.05511 | 28.61094 | 484 | 33.2 | 800 |
| 16 | Governmental | Omm Kheleef | $S_3$ | 28.09428 | 28.60564 | 460 | 30.3 | 600 |

(--): Not Applied

The chemistry of geothermal waters varies depending on the source of recharge waters and the contribution of gases from magmatic or metamorphic sources. The majority of geothermometers are based on

specific chemical equilibrium reactions and the system's nature. As geothermal waters rise from a deep reservoir to the surface, they may cool due to conductive heat loss as they pass through cooler rocks.

The chemical and isotopic composition of the water is unaffected by conduction cooling. Whereas, the saturation state of some minerals might be altered , which in turn, can change the chemical composition of the upward water (Karingithi, 2009).

The position of water samples in the Cl-$SO_4$-$HCO_3$ ternary diagram (Fig. 4a) is mostly plotted toward the $SO_4$ and Cl corners in the field of steam heated or volcanic waters. This reflects the dominance of $SO_4$, Cl–rich waters , despite they are all of fresh water types. This could be referred to the dissolution of marine deposits, which percolate through faults into the deep geothermal water as well as the ion exchange processes. On the other hand, samples were plotted in the immature waters area in the Na-K-Mg ternary diagram (Fig. 4b). They are located close to the Sqrt.(Mg) corner, which suggests the regular interaction between water and the host rocks in the geothermal system.

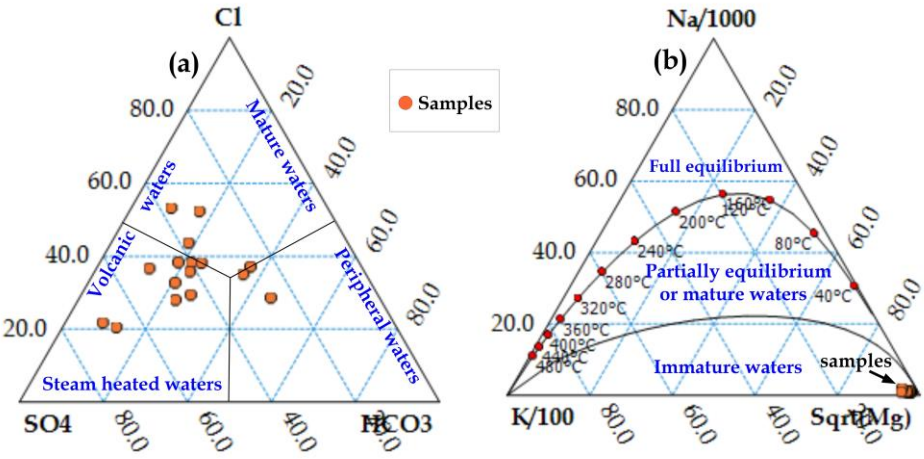


**Fig. (4). a.** Cl–$SO_4$–$HCO_3$ ternary diagram, **b.** Giggenbach Na–K–Mg triangle.

The subsurface temperatures were further calculated based on different geothermometers (Table 2). The results showed that the silica geothermometer, according to Fournier (1977), gave much more realistic temperatures (29-54ºC), which were slightly higher than the field-measured temperatures (26.7-46.4ºC). Moreover, the K/Mg geothermometry calculations, (Giggenbach, 1988), gave lower reservoir temperatures (16-33°C). The proper explanation for that is the change of the reservoir temperature due to mixing between the shallower cold water and the deep

thermal groundwater as a result of the downward slow flow. The Na/K calculations, based on Fournier (1979) and Giggenbach (1988), have much higher temperatures for thermal waters with reservoir temperature ranges of (235-299ºC) and (244-346ºC), respectively. This could be interpreted because of the (Na/K) ratio is mainly based on temperature dependent cation exchange reaction between albite and K feldspar. Moreover, the Na-K geothermometer gives poor results below 100°C (Karingithi, 2009).

**Table (1).** Calculations of the temperature (°C) of the multilayered aquifer by different geothermometers

| Well | Measured temperature | (a) Silica (quartz), (Fournier, 1977) | (b) K-Mg (Geggenbach, 1988) | (c) Na-K (Giggenbach, 1988) | (d) Na-K (Fournier, 1979) |
|---|---|---|---|---|---|
| 1 | 30.2 | 33 | 29 | 246 | 237 |
| 2 | 26.7 | 39 | 24 | 296 | 293 |
| 3 | 29.8 | 37 | 23 | 298 | 295 |
| 4 | 29.7 | 29 | 33 | 265 | 258 |
| 5 | 27.3 | 40 | 19 | 244 | 235 |
| 6 | 27.7 | 36 | 24 | 292 | 289 |
| 7 | 28.3 | 47 | 16 | 346 | 350 |
| 8 | 30.2 | 35 | 28 | 271 | 265 |
| 9 | 29.7 | 41 | 29 | 276 | 270 |
| 10 | 28.3 | 39 | 24 | 257 | 249 |
| 11 | 29.8 | 46 | 27 | 272 | 266 |
| 12 | 30.1 | 46 | 27 | 272 | 266 |
| 13 | 46.4 | 54 | 27 | 301 | 299 |
| 14 | 30 | 39 | 30 | 270 | 264 |
| 15 | 33.2 | 30 | 29 | 246 | 237 |
| 16 | 30.3 | 37 | 28 | 260 | 253 |

(a) T = {1309/[5.19-Log(SiO2)]}-273.15
(b) T = {4410/[14-Log(K2/Mg)]}-273.15
(c) T = {1390/[1.750-Log(Na/K)]}-273.15
(d) T = {1217/[1.438-Log(Na/K)]}-273.15
*units used in equations (a) and (b) are mg/l, while mmol/l units were applied in equations (c) and (d)

The concentrations of major ions, environmental isotopes, as well as some trace elements and chemical water types are grouped in Table (3).The ranges of the total dissolved solids (TDS) are 160 mg/l and 554 mg/l, with a mean value of 268 mg/l, indicating fresh water types according to Freeze and Cherry (1979); the majority of the samples showed salinity below 300 mg/l, (Fig. 5a, b and c). The ranges of the major ions in mg/l (Table 3),

**Table (3).** Water types, chemical and isotopic analysis data for the studied groundwater samples.

| ID | Water type | pH | Concentrations in mg/l | | | | | | | | | | | | $\delta^{18}O$‰ | $\delta D$‰ |
|---|---|---|---|---|---|---|---|---|---|---|---|---|---|---|---|---|
| | | | TDS | Ca | Mg | Na | K | $CO_3$ | $HCO_3$ | $SO_4$ | Cl | $SiO_2$ | Al | Fe | Mn | | |
| 1 | Na-Mg-$SO_4$ | 5.94 | 367 | 32.0 | 24.30 | 50.0 | 10.0 | 0.0 | 24.4 | 182.14 | 56.60 | 8.23 | 0.00 | 11.03 | 0.95 | -6.11 | -65.7 |
| 2 | Ca-Na-Mg-$SO_4$-Cl | 6.31 | 236 | 26.0 | 14.58 | 29.0 | 10.6 | 0.0 | 36.6 | 81.00 | 56.60 | 10.03 | 0.00 | 8.48 | 0.63 | -- | -- |
| 3 | Ca-$SO_4$ | 5.99 | 376 | 48.0 | 19.44 | 35.0 | 12.3 | 0.0 | 36.6 | 186.00 | 56.60 | 9.30 | 0.06 | 9.26 | 0.84 | -6.40 | -58.70 |
| 4 | Na-Mg-Ca-Cl-$SO_4$ | 6.44 | 149 | 16.0 | 9.72 | 20.0 | 5.0 | 0.0 | 24.4 | 44.00 | 42.00 | 7.18 | 0.22 | 9.31 | 0.40 | -- | -- |
| 5 | Na-Cl-$SO_4$ | 6.74 | 544 | 35.0 | 31.90 | 102.0 | 20.0 | 0.0 | 36.6 | 138.84 | 198.11 | 10.23 | 0.06 | 8.11 | 0.54 | -2.28 | -48.63 |
| 6 | Ca-Na-Cl-$SO_4$ | 5.79 | 199 | 27.0 | 9.72 | 24.0 | 8.0 | 0.0 | 27.4 | 62.00 | 55.00 | 9.14 | 0.13 | 7.54 | 0.37 | -5.29 | -59.99 |
| 7 | Mg-Cl | 6.20 | 402 | 32.0 | 35.50 | 46.0 | 25.0 | 0.0 | 48.8 | 89.00 | 150.00 | 12.57 | 0.27 | 9.62 | 1.54 | -5.32 | -59.15 |
| 8 | Na-Mg-$SO_4$-Cl | 6.44 | 200 | 15.0 | 15.00 | 32.0 | 8.0 | 0.0 | 34.6 | 72.00 | 41.00 | 8.79 | 0.00 | 7.00 | 0.33 | -- | -- |
| 9 | Na-Mg-Ca-$SO_4$-Cl | 6.45 | 189 | 20.0 | 12.15 | 25.0 | 7.0 | 0.0 | 38.0 | 64.00 | 42.00 | 10.43 | 0.09 | 8.66 | 0.32 | -5.05 | -55.95 |
| 10 | Na-Cl-$SO_4$ | 6.48 | 212 | 18.0 | 9.72 | 35.0 | 8.0 | 0.0 | 36.6 | 66.00 | 56.60 | 9.79 | 0.18 | 6.40 | 0.35 | -- | -- |
| 11 | Na-Ca-Cl | 6.49 | 173 | 19.0 | 9.72 | 26.0 | 7.0 | 0.0 | 48.8 | 39.40 | 47.17 | 12.31 | 0.18 | 7.21 | 0.30 | -4.1 | -54.84 |
| 12 | Na-Ca-Cl | 6.56 | 169 | 18.0 | 9.72 | 26.0 | 7.0 | 0.0 | 48.8 | 35.00 | 49.00 | 12.44 | 0.15 | 7.41 | 0.33 | -- | -- |
| 13 | Mg-Na-Cl-$HCO_3$ | 6.65 | 159 | 14.0 | 12.40 | 22.0 | 8.0 | 0.0 | 61.0 | 34.30 | 37.74 | 15.49 | 0.09 | 3.87 | 0.56 | -9.84 | -79.9 |
| 14 | Ca-Cl-$SO_4$ | 6.33 | 200 | 32.0 | 9.72 | 22.0 | 5.8 | 0.0 | 36.6 | 56.00 | 56.60 | 9.83 | 0.29 | 12.84 | 0.72 | -- | -- |
| 15 | Na-$SO_4$-Cl | 5.77 | 267 | 26.0 | 15.40 | 40.0 | 8.0 | 0.0 | 24.4 | 96.00 | 69.00 | 7.45 | 0.00 | 18.24 | 1.05 | -8.09 | -74.6 |
| 16 | Na-Mg-Cl-$SO_4$ | 6.00 | 268 | 24.0 | 19.44 | 38.0 | 9.0 | 0.0 | 36.6 | 74.00 | 84.91 | 9.38 | 0.00 | 9.43 | 0.91 | -7.07 | -64.91 |
| Min | | 5.77 | 149 | 14.0 | 9.72 | 20.0 | 5.0 | 0.0 | 24.4 | 34.30 | 37.74 | 7.18 | 0.00 | 3.87 | 0.30 | -9.84 | -79.90 |
| Max. | | 6.74 | 544 | 48.0 | 35.50 | 102.0 | 25.0 | 0.0 | 61.0 | 186.00 | 198.11 | 15.49 | 0.29 | 18.24 | 1.54 | -2.28 | -48.63 |
| Mean | | 6.3 | 257 | 25.1 | 16.2 | 35.8 | 9.9 | 0.0 | 37.5 | 82.50 | 68.7 | 10.2 | 0.1 | 9.0 | 0.6 | -6.0 | -62.2 |
| WHO maximum guidelines | | 6.6-8.5 | 1000 | 300 | 150 | 200 | 30 | -- | 300 | 250 | 250 | -- | 0.1-0.2 | 0.3 | 0.02-.08 | -- | -- |

(--): Not Applied

including Ca (14-48; Avg. 21), Mg (10-36; Avg. 16), Na (20-102; Avg. 36), K (5-25; Avg. 10), $HCO_3$ (24-61; Avg. 38), $SO_4$ (34-186; Avg. 83) and Cl (38-198; Avg. 69), showed that they fall within the World Health Organization (WHO 2022) limits for drinking.

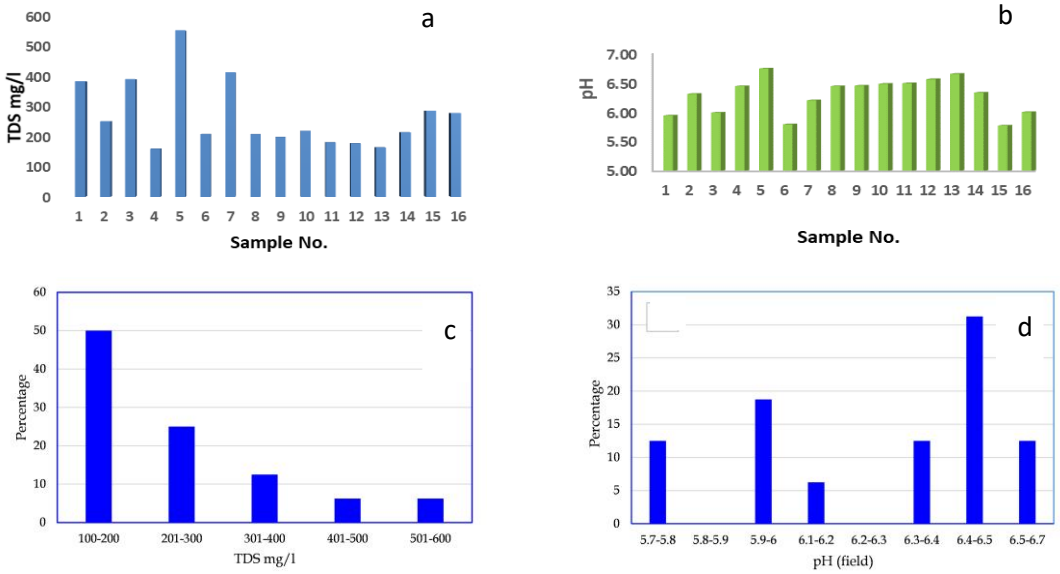


**Fig. (5).** Salinity and pH distribution for the studied groundwater samples.

As for some trace elements, such as aluminum (Al), iron (Fe) and manganese (Mn), their values ranged from (0-0.29; Avg. 0.1 mg/l), (3.9-19; Avg. 9 mg/l) and (0.3-1.5; Avg. 0.6 mg/l), respectively. This imply that Al is falling within the ranges of WHO limits for almost all the studied groundwater samples, while the Fe and Mn concentrations exceeded the maximum limits indicating that these two elements sourced mainly as a result of the interaction of groundwater with the sediments rich in iron and manganese. It is worth mentioning that the iron concentration is reached its maximum values in the groundwater samples abstracted from layer $S_2$, which was indicated by Sharaky and Abdoun (2020) as a ferruginous sandstone water bearing zone.

Water samples show quite low pH values ranging from 5.77 to 6.74 with an average value of 6.29, reflecting acidic to slightly acidic waters. Most of the samples' pH values are ranging from 6.4 to 6.5 (Fig. 5b and d). The decrease in the pH values in the studied groundwater samples, that makes groundwater weakly acidic or acidic can be explained in the light of different factors such as: (i) the formation of $H_2CO_3$ as a result of $CO_2$ solvation, which in turn dissociates and causing an increase in $HCO_3$ and a decrease in pH in groundwater (Isa et al., 2012); (ii) The oxidation of pyrite

in sediments reduce the concentration of pH in groundwater (Preda and Cox, 2000); (iii) According to Sjöström (1993), clay minerals may serve as $H^+$ buffers and affect the pH of groundwater. The last two assumptions are probably the case here, since the aquifer matrix is mainly composed of alternative ferruginous sandstone and clay layers. This could be explained as a result of the reaction of the dissolved iron with oxygen present in the infiltrating waters, which is thought to be the main cause of the low pH values (Degens and Shand, 2010). The pH remains low, especially when neutralizing minerals like carbonates are absent from aquifers. However, neutralizing minerals, such as carbonates, frequently react where they are present to reduce the impact on pH. Additionally, when waters lack oxygen, as in the deep aquifers, microbial attack can dissolve iron oxides producing alkalinity (often in the form of dissolved bicarbonate).

**1.1. Geochemical processes**

**1.1.2. Hydrochemical facies and evolution**

The hydrochemical water types of the studied groundwater samples (Table 3) revealed that almost all the samples are dominated by Na followed by Mg and Ca, while the prevailing anions are Cl, $SO_4$ followed by $HCO_3$. The primary hydrochemical facies the numerous operations that govern groundwater chemistry could be also illustrated by plotting the constituents of the analyzed water samples on both the Piper (Piper, 1944) and Chadha (Chadha, 1999) diagrams. Based on the location of water samples in certain sub areas of the diamond-shaped field of the Piper's graph (Fig. 6a), three groundwater types can be distinguished; Na-Cl type, Ca-Cl type and mixed Ca-Mg-Cl type, which is predominated in the study area. The projection of the water points revealed the impact of different processes on the groundwater chemistry, where most of the samples are located in the mixed type area. It is obvious that the general trend of water types is changing from Ca-Sodium-$HCO_3$ waters to Ca-sodium-$SO_4$-Chloride water types. This groundwater is significantly dominated by Ca and Na over Mg and K and by strong acids ($SO_4$ + Cl) over weak acids ($CO_3$ + $HCO_3$). This reflects the effect of the leaching and dissolution of marine sediment, (referred in section 2), as well as the cation exchange processes (Fig. 6b). It is important to note that the change in chemical composition makes the samples deviate upward into the upper right portion of the diamond shape during leaching with aquifer matrix and the cation-exchange process, while being deviated to the middle part toward diamond's center is because of the mixing processes (Appelo and Postma, 2004).

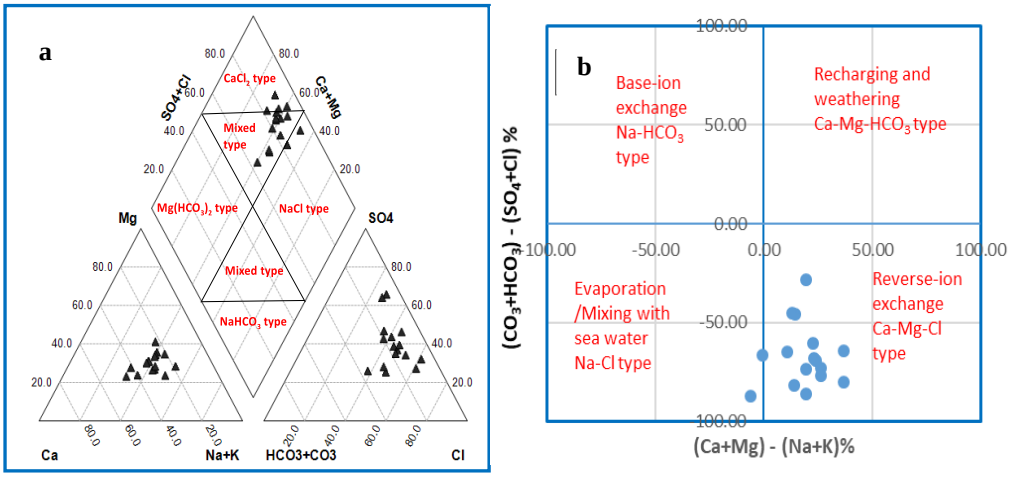


**Fig. (6). a.** Piper diagram showing the different hydrochemical facies, while Chadha diagram, **b.** An illustration on the classification and different processes affecting groundwaters.

To distinguish between the rock-water interaction and the sources of dissolved ions, such as precipitation, rock weathering, and evaporation, all of which have an impact on the water chemistry, Gibbs diagram has been used (Gibbs, 1970). The sample positions (Fig. 7) revealed that most of the samples were compiled in areas where rocks predominated, indicating that weathering and rock dissolution were the primary factors influencing the hydrochemistry of the groundwater.

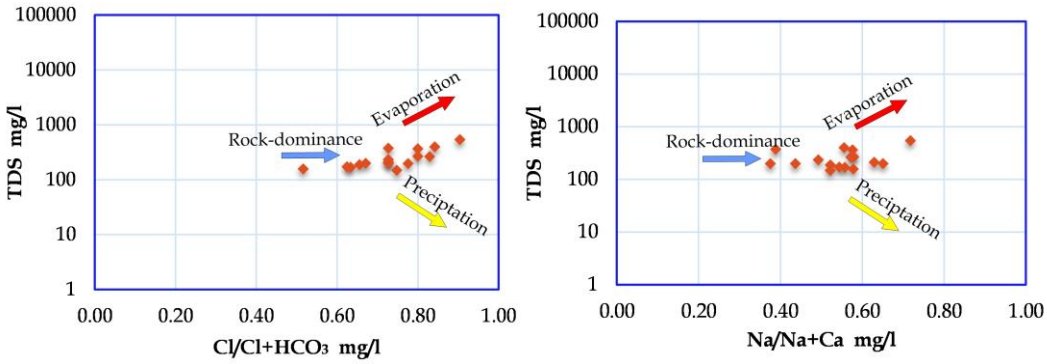


**Fig. (7).** Gibbs diagram showing that the rock-water interaction is the geochemical processes.

### 5.1.1. Correlation coefficients (ion ratios relationships)

The various possible processes, such as leaching, ion exchange, evaporation and mixing with surface waters such as seawater that could be involved in the development of the chemistry of groundwater are outlined by a number of major ion scatter plots (Hounslow, 2018). The Na/Cl versus Ca/Mg scatter plot (Fig. 8a) shows that most of the samples are affected by reverse ion exchange that release Ca and Mg into solution and the adsorption of Na on clays as well as calcite and dolomite dissolution with a minor impact of the faster groundwater circulation.

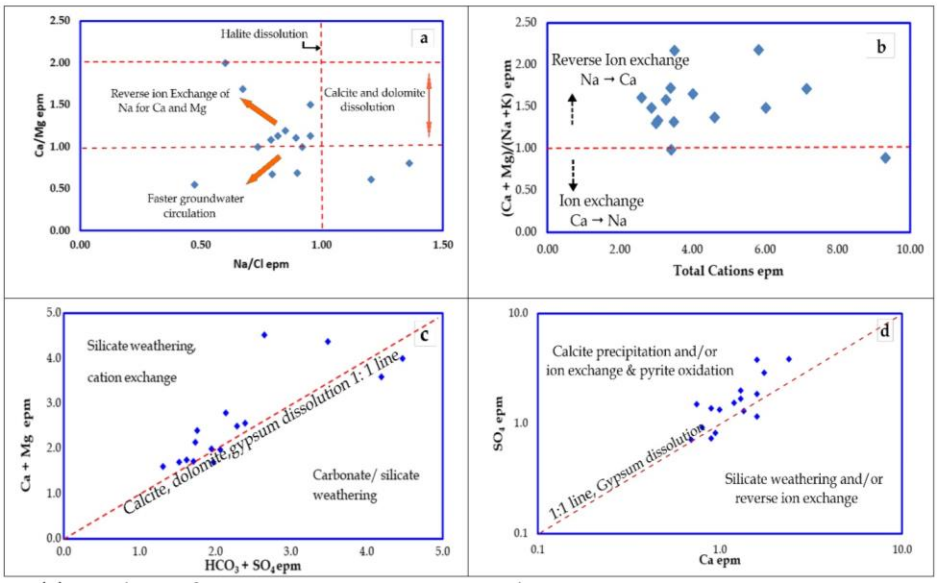


**Fig. (8).** Correlation of some ionic parameters on scatter plots.

The total cations against Ca+Mg/Na+K relationship is mainly used to interpret the impact of the ion exchange processes on groundwater chemistry. The position of the samples on this plot indicated the dominance of the reverse ion exchange processes (Fig. 8b). Additionally, the distribution of the sample positions on the Ca+Mg against the $HCO_3$+$SO_4$ scatter plot (Fig. 8c) appeared on, above, and below the 1:1 line, indicating that the primary sources of these ions are weathering of carbonates and silicates, as well as the dissolution of calcite, dolomite, and gypsum. (Fisher and Mullican, 1997; Ezzeldin, 2022 and Masoud et al., 2023). The Ca/$SO_4$ correlation (Fig. 8d) demonstrated that most of the samples were plotted above the 1:1 line. This is probably due to the removal of calcium by calcite precipitation, or cation exchange and pyrite oxidation. On the other hand, the minority of the samples fall below the 1:1 line. This indicates that the dissolution of gypsum is a secondary process and other reactions take place such as silicate weathering, since the $HCO_3$ is greater

than $SiO_2$ and the TDS is low in all samples (Hounslow, 2018). Additionally, a few samples were located on the 1:1 line, indicating gypsum dissolution.

The saturation indices (SIs) of some proposed minerals were determined to gain a greater understanding of the interaction of rocks with circulating groundwater (Parkhurst and Appelo, 2013). The chemical analysis data as well as the subsurface geology background are utilized to select these minerals. Fig. (9) depicts the SI measured values of the selected minerals. The figure illustrates halite dissolution with negative SI values, whereas iron minerals (siderite and hematite) are supersaturated with apparent positively values. Carbonate minerals (calcite and dolomite), as well as sulphates (anhydrite and gypsum), are insufficiently soluble in groundwater, with values that fluctuate positively and negatively around zero. This confirms the role of the various geochemical processes, which were previously identified by studying the relationships of ions with each other, in either the enrichment or depletion of groundwater with the elements related to these minerals.

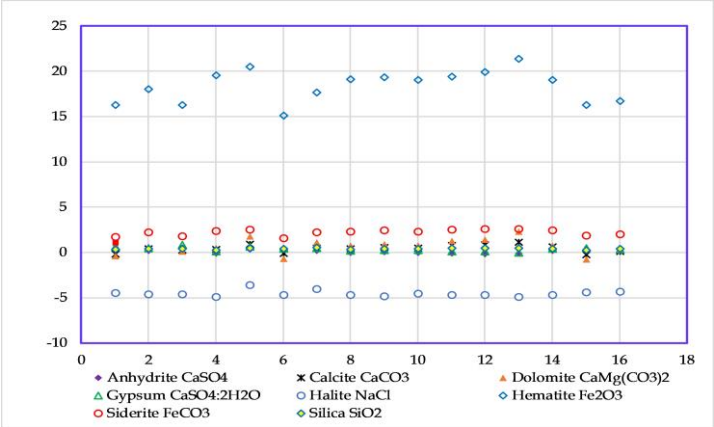


**Fig. (9).** Computed saturation indices (SI) for the studied groundwater samples.

### 5.2. Statistical analysis (Factor Analysis)

Factor analysis (FA) was used to describe the factors impacted the groundwater chemistry. A subset of 13 water quality indicators, including pH, TDS, Ca, Mg, Na, K, $HCO_3$, $SO_4$, Cl, Al, Fe, $^{18}O$ and D were used in this analysis. When SPSS program is applied, three factors that accounted for 82.76% of the variations were discovered (Table 4).

**Table (4).** Rotated Component Matrix.

| Component | F1 | F2 | F3 |
|---|---|---|---|
| pH | 0.22 | 0.82 | 0.35 |
| TDS | 0.96 | -0.23 | 0.04 |
| Ca | 0.64 | -0.53 | -0.05 |
| Mg | 0.94 | -0.02 | -0.09 |
| Na | 0.87 | -0.09 | 0.20 |
| K | 0.91 | 0.18 | -0.07 |
| $HCO_3$ | -0.03 | 0.95 | -0.19 |
| $SO_4$ | 0.57 | -0.61 | -0.04 |
| Cl | 0.92 | 0.11 | 0.11 |
| $SiO_2$ | -0.05 | 0.97 | -0.17 |
| Fe | 0.05 | -0.78 | -0.16 |
| $O^{18}$ | 0.50 | -0.04 | 0.74 |
| D | -0.20 | 0.06 | 0.86 |
| Total eigen value | 5.64 | 3.62 | 1.50 |
| Total variance % | 40.91 | 29.84 | 12.01 |
| Cumulative % | 40.91 | 70.75 | 82.76 |

Extraction method: Principal Component Analysis.
Rotation method: Varimax with Kaiser Normalization.

Factor 1, which accounts for 40.91% of the total variance and 5.64 of the total eigen value, was found to have strong positive loadings with TDS, Ca, Mg, Na, K, and Cl, as well as moderate positive loadings with $SO_4$. As a result, this factor indicates that salinity is highly correlated with the major ions in groundwater, indicating the role of rock-water interaction in groundwater chemistry.

The second factor ($F_2$), which accounts for 29.4% of total variance and 3.62 of total eigenvalue, is related to significant positive loadings with pH, $HCO_3$, and $SiO_2$, as well as strong negative loading values with Fe and $SO_4$. As a result, $F_2$ is claimed to be an indicator of the silicate and carbonate weathering processes that were previously confirmed in the section on ionic relations. The negative loadings of this factor with Fe, Ca, and $SO_4$ on the other hand explain the precipitation of iron minerals such as hematite and siderite, which is consistent with the previously calculated saturated indices.

Factor 3 accounts for 12.01% of total variance and 1.5 of total eigenvalue, and it is distinguished by significant positive loadings with $O^{18}$ and deuterium, indicating the mixing of deep geothermal water (in the $S_1$ layer) with shallower water in zone $S_3$. The first ($F_1$), second ($F_2$), and third ($F_3$) factors define the spatial distributions of the variables in the spaces (Fig. 10).

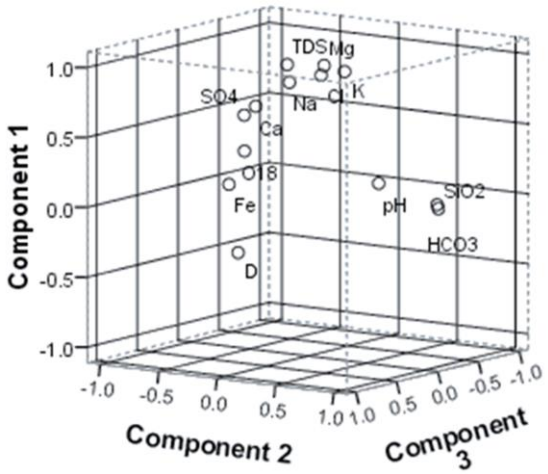


**Fig. (10)**. 3D representation of loadings of factor 1, factor 2, and factor 3 after varimax rotation.

### 5.3. Stable isotopes

The stable isotopic data are summarized in table 3. They ranged from -9.84 to -2.28 (on average -6.0) and from -79.90 to -48.63 (on average -62.20) for $\delta^{18}O$ and D, respectively. The oxygen-18 against deuterium plot (Fig. 11a) shows that samples were plotted below and to the right of the GMWL (Craig, 1961), indicating the influence of paleowater with depleted values when compared to recent water.

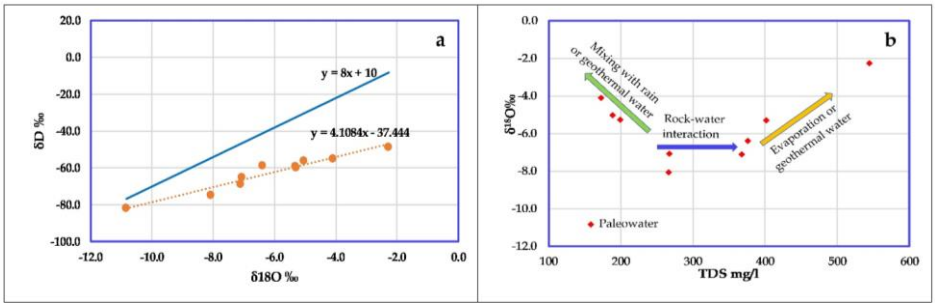


**Fig. (11). a.** $\delta^{18}O$ versus Δd, **b.** Total dissolved solids versus $\delta^{18}O$ for the studied groundwater samples.

It should be noted that all samples plot on the evaporation line whilst still having lower $^{18}O$ and D values than modern groundwaters, implying that some groundwater was recharged during glacial periods during the Pleistocene. Another plausible explanation of the relatively enrichment of the isotopic content is due to the fractionation effect caused by the passage

of water through micro-pores in shales, clays or other semipermeable materials ( Graf et al., 1965 and Hitchon and Friedman, 1969). In a bivariate plot (Fig. 11b), the variation in "$\delta^{18}O$" composition is also correlated with TDS to show how various processes have an impact on groundwater. According to the position of the groundwater samples on this plot, they can be divided into three groups. One group, which was enriched in its isotopic content and had a slightly higher salinity (>400 mg/l), was subjected to evaporation or geothermal activity. A second group, which had an enrichment in isotopes and a much lower salinity (300 mg/l), indicated that recent and geothermal waters had been mixed. The remaining group described the impact of the interaction between rocks and water, where the isotopic composition remains constant as salinity rises.

## CONCLUSION

The current study demonstrated the significance of using major ion chemistry, geochemical modelling calculations, statistical analysis, and stable isotope tools to pinpoint the variables influencing groundwater quality in the El-Heiz area, south of El-Bahrayia Oasis.

Based on the location of water samples in Piper and Chadha graphs, three groundwater types can be distinguished; Na-Cl type, Ca-Cl type and mixed type. Additionally, the majority of groundwaters are dominated by the reverse exchange processes, which lead to the increase of Na ion at the expense of both Ca and Mg ions. Moreover, the sample positions on Gibbs diagram indicated that weathering and rock dissolution were the primary factors influencing the hydrochemistry of the groundwater.

The application of SPSS and PHREEQC programs, along with the ion correlation coefficients revealed that there are three factors impacted groundwater mineralization. These determinants impacted the groundwater geochemistry include, the rock-water interaction, carbonate and silicate-weathering mechanisms, ion-exchange as well as evaporation and/or mixing with deep geothermal waters.

Finally, the stable isotopes ($\delta^{18}O$ and $\delta D$) indicated that the groundwater abstracted from the Nubian Sandstone Aquifer (NSA) is mainly recharged from the paleo-water, which was subjected to leaching, dissolution and geothermal activities.

## REFERENCES

Abd El-Latif, R. (2007). Study of groundwater resources management in Bahariya Oasis. Ph.D. Thesis, Fac. Sci., Alexandria University, Egypt.

Abdel Ati, A. (1995). Groundwater conditions in El Bahariya Oasis and future development. M.Sc. Thesis, Faculty of Science, Cairo University, Egypt.

Appelo, C.A.J. and D. Postma (2004). In: 'Geochemistry, Groundwater and Pollution'. CRC Press.

American Society for Testing Materials (1999). Annual Book of ASTM Standards, 6.

Back, W. (1960). Hydrochemical facies and ground-water flow patterns in Northern Atlantic Coastal Plain. AAPG Bulletin, 44: 1244-1245.

Chadha, D. (1999). A proposed new diagram for geochemical classification of natural waters and interpretation of chemical data. Hydrogeology Journal, 7: 431-439.

Conoco, C. (1987). Geological map of Egypt, scale 1: 500,000-NF 36 NE-Bernice, Egypt. The Egyptian General Petroleum Corporation, Cairo.

Craig, H. (1961). Isotopic variations in meteoric waters. Science, 133: 1702-1703.

Degens, B. and P. Shand (2010). Assessment of Acidic Saline Groundwater Hazard in the Western Australian Wheatbelt: Yarra Yarra, Blackwood and South Coast. CSIRO Water for a Healthy Country National Research Flagship, 152 p.

Diab, M. (1972). Hydrogeological and hydrochemical studies of the Nubian Sandstone water-bearing complex in some localities in United Arab Republic. Ph.D. Thesis, Assiut University, Assiut, Egypt.

El Akkad, S. and B. Issawi (1963). Geology and iron ore deposits of the Bahariya Oasis. Geological Survey and Mineral Resources Dept., Cairo, 18, 301 p. US Government Printing Office.

Embabi, N.S. and M.A. El Kayali (1979). A morpho-tectonic map of the Bahariya Depression. Ann. Geol. Surv. Egypt, VIX: 179–183.

Ezzeldin, H.A. (2022). Delineation of salinization and recharge sources affecting groundwater quality using chemical and isotopic indices in the Northwest Coast, Egypt. Sustainability, 14: 16923.

Fisher, R.S. and I.W. Mullican (1997). Hydrochemical evolution of sodium-sulfate and sodium-chloride groundwater beneath the northern Chihuahuan Desert, Trans-Pecos, Texas, USA. Hydrogeology Journal, 5: 4-16.

Fishman, M.J. and L.C. Friedman (1989). In: "Methods for Determination of Inorganic Substances in Water and Fluvial Sediments," US Geological Survey Techniques of WaterResources Investigations, Book 5, Chapter A1.

Foster, S. and D.P. Loucks (2006). In: 'Non-Renewable Groundwater Resources: A Guidebook on Socially-Sustainable Management for Water-Policy Makers'. Unesco, Paris, France, 103 p.

Fournier, R.O. (1977). Chemical geothermometers and mixing models for geothermal systems. Geothermics, 5: 41-50.

Fournier, R.O. (1979). A revised equation for the Na/K geothermometer. GRC Transactions, 3: 221-224.

Freeze, R.A. and J.A. Cherry (1979). Groundwater. Prentice-Hall Inc. Englewood Cliffs, Vol. 7632, New Jersy, 604 p.

Gibbs, R.J. (1970). Mechanisms controlling world water chemistry. Science, 170: 1088-1090.

Giggenbach, W.F. (1988). Geothermal solute equilibria. derivation of Na-K-Mg-Ca geoindicators. Geochimica et Cosmochimica Acta, 52: 2749-2765.

Giggenbach, W. (1991). Chemical techniques in geothermal exploration. In: 'Application of Geochemistry in Geothermal Reservoir Development', pp. 119-144.

Graf, D.L., I. Friedman and W.F. Meents (1965). In: 'The Origin of Saline Formation Waters, II: Isotopic Fractionation by Shale Micropore Systems'. Circular no. 393.

Gupta, R.P., R.K. Tiwari, V. Saini and N. Srivastava (2013). A simplified approach for interpreting principal component images. Advances in Remote Sensing, 2 (2): 111-119.

Hamdan, A.M. and R.F. Sawires (2013). Hydrogeological studies on the Nubian sandstone aquifer in El-Bahariya oasis, Western Desert, Egypt. Arabian Journal of Geosciences, 6: 1333-1347.

Han, D., X. Liang, M. Jin, M. Currell, X. Song and C. Liu (2010). Evaluation of groundwater hydrochemical characteristics and mixing behavior in the Daying and Qicun geothermal systems, Xinzhou Basin. Journal of Volcanology and Geothermal Research, 189: 92-104.

Himida, I. (1964). Artesian water of the oases of Libyan Desert in UAR. Ph.D. Thesis, MGRU, Moscow, Russia.

Hitchon, B. and I. Friedman (1969). Geochemistry and origin of formation waters in the western Canada sedimentary basin—I. Stable isotopes of hydrogen and oxygen. Geochimica et Cosmochimica Acta, 33: 1321-1349.

Hounslow, A.W. (2018). In: 'Water Quality Data: Analysis and Interpretation'. CRC Press.

Isa, N.M., A.Z. Aris and W.N.A.W. Sulaiman (2012). Extent and severity of groundwater contamination based on hydrochemistry mechanism of sandy tropical coastal aquifer. Science of the Total Environment, 438: 414-425.

Karingithi, C.W. (2009). Chemical geothermometers for geothermal exploration. Presented at Short Course IV on Exploration for Geothermal Resources, UNU-GTP, KenGen and GDC, Lake Naivasha, Kenya

Khalifa, R. (2006). In: 'Study of Groundwater Resources Management in El-Bahariya Oasis'. Alexandria University, Alexandria, Egypt.

Khazaei, E., R. Mackay and J.W. Warner (2004). The effects of urbanization on groundwater quantity and quality in the Zahedan aquifer, southeast Iran. Water international, 29: 178-188.

Masoud, M., M. El Osta, A. Alqarawy and H. Ezzeldin (2023). Application of environmental isotopes and hydrochemistry to identify the groundwater recharge in Wadi Qanunah Basin, Saudi Arabia. Sustainability, 15: 2648.

Ministry of Public Works and Water Resources (1998). Hydrogeology of deep aquifers in the Western Desert and Sinai; Water Policy Reform Program, International Resources Group Winrock International, Nile Consultants, Report No. 10, Available online: http://iwrm2eg.org/report/ Epiqreport/Report10APRP.pdf.

Parkhurst, D.L. and C. Appelo (2013). Description of input and examples for PHREEQC version 3—a computer program for speciation, batch-reaction, one-dimensional transport, and inverse geochemical calculations. US Geological Survey Techniques and Methods, 6: 497.

Piper, A.M. (1944). A graphic procedure in the geochemical interpretation of water-analyses. Eos, Transactions American Geophysical Union, 25: 914-928.

Pirlo, M.C. (2004). Hydrogeochemistry and geothermometry of thermal groundwaters from the Birdsville Track Ridge, Great Artesian Basin, South Australia. Geothermics, 33: 743-774.

Polemio, M., D. Casarano and P.P. Limoni (2009). Karstic aquifer vulnerability assessment methods and results at a test site (Apulia, southern Italy). Natural Hazards and Earth System Sciences, 9: 1461-1470.

Preda, M. and M. Cox (2000). Sediment–water interaction, acidity and other water quality parameters in a subtropical setting, Pimpama River, southeast Queensland. Environmental Geology, 39: 319-329.

Prior, J.C., J.L. Boekhoff, M.R. Howes, R.D. Libra and P.E. VanDorpe (2003). In: 'Iowa's Groundwater Basics'. Iowa Department of Natural Resources. First edition. Iowa, India.

RIGW (Research Institute for Groundwater) (2010). Hydrogeological map of El-Bahariya Oasis; Scale 1:100,000 Project. Hydrogeologcal maps of the Western Desert Development Areas, Egypt. Internal Report, RIGW, Egypt.

Seaber, P. (1962). Cation hydrochemical facies of groundwater in the Englishtown Formation, New Jersey. US Geological Survey Professional Paper, 450: 124-126.

Sharaky, A. and S.H. Abdoun (2020). Assessment of groundwater quality in Bahariya Oasis, Western Desert, Egypt. Environmental Earth Sciences, 79: 1-14.

Sjöström, J. (1993). Ionic composition and mineral equilibria of acidic groundwater on the west coast of Sweden. Environmental Geology, 21: 219-226.

Stober, I. (2013). Geothermal fluid and reservoir properties in the Upper Rhine Graben, Europe. In Second EAGE Sustainable Earth Sciences (SES) Conference and Exhibition, cp-361-00024. EAGE Publications BV.

Su, S., Y. Li Z. Chen, Q. Chen, Z. Liu, C. Lu and L. Hu (2022). Geochemistry of geothermal fluids in the Zhangjiakou-Penglai Fault Zone, North China: Implications for structural segmentation. Journal of Asian Earth Sciences, 230: 105218.

World Health Organization, W.H.O. (2022). Guidelines for drinking-water quality: fourth edition incorporating the first and second addenda. Available online: https://apps.who.int/iris/rest/bitstreams/1414381/retrieve

Zaporozec, A. (1972) groundwater zoning in water resources management 1. Jawra Journal of the American Water Resources Association, 8: 1137-1143.

Zeng, X. and T.C. Rasmussen (2005) Multivariate statistical characterization of water quality in Lake Lanier, Georgia, USA. Journal of Environmental quality, 34: 1980-1991.

# استقصاء المياه الجوفية باستخدام منهجية هيدروجيوكيميائية بمنطقة الحيز، الواحات البحرية، الصحراء الغربية، مصر

**محمد أحمد جمعة، جيلان عبد الوهاب عمر، هشام عبد الحميد عزالدين*، يسرا حافظ قطب وسعد أحمد مهلل**

قسم الهيدروجيوكيمياء، مركز بحوث الصحراء، المطرية، القاهرة، مصر

تتميز منطقة الحيز، وهي جزء من الواحات البحرية، بتواجد خزان الحجر الرملي النوبي غير المتجدد والذي يحتوي على كميات كبيرة من المياه العذبة. تم جمع عدد ١٦ عينة من المياه الجوفية ممثلة لطبقات خزان الحجر الرملي النوبي المختلفة (NSA)، بغرض قياس بعض الخواص الفيزيائية وكذلك لإجراء بعض التحاليل الكيميائية والنظائرية. أشارت القيم المتوسطة لمجموع الأملاح الذائبة (TDS) لعينات المياه إلى أن جميعها تعتبر مياه عذبة، حيث تراوحت هذه القيم ما بين ١٤٩ مجم/لتر و٥٤٤ مجم / لتر بمتوسط ٢٥٧ مجم/ لتر. ومع ذلك، أظهرت قيم الأس الهيدروجيني المقاسة بأن المياه حمضية نسبيًا حيث تراوحت قيمها من ٥.٧٧ إلى ٦.٧٤ بمتوسط ٦.٣. كما تباينت درجات الحرارة المقاسة بشكل كبير، نتيجة اختلاف اعماق الآبار، وتراوحت درجات الحرارة من ٢٦.٣ درجة مئوية إلى ٤٦.٤ درجة مئوية. أظهرت قيم النظائر الثابتة المقاسة (مثل الاكسجين-١٨ و الديوتيريوم) تباينًا في المحتوى النظائري، حيث تراوحت من ٩.٨٤- إلى ٢.٢٨- (بمتوسط ٦.٠-) ومن ٧٩.٩– إلى ٤٨.٦٣- (بمتوسط ٦٢.٢-) لكل من الأكسجين-١٨ والديوتيريوم، على الترتيب. يشير التباين الكبير في قيم النظائر الثابتة إلى دور العمليات الجيوكيميائية المختلفة التي يمكن أن تؤثر على نوعية المياه الجوفية. أظهرت نتائج بعض العناصر الشحيحة مثل الحديد والمنجنيز قيمًا تجاوزت الحد المسموح به لأغراض الشرب في بعض عينات المياه الجوفية المدروسة. تم تطبيق برنامج PHREEQC لحساب مؤشرات التشبع لبعض المعادن المختارة مثل الأنهيدريت والجبس والهاليت والكالسيت والدولوميت والسيدريت والهيماتيت لتحديد دور العملية الجيوكيميائية في تطور نوعية المياه الجوفية. أشارت نتائج التحاليل الإحصائية إلى وجود ثلاثة عوامل أثرت على المياه الجوفية، بما في ذلك التبخر وكذلك تأثير المياه الجوفية العميقة الحارة، إضافة إلى عمليات التفاعل بين الصخور والمياه، وعمليات التبادل الأيوني. بشكل عام، أظهرت النتائج أن المياه الجوفية المستخرجة من خزان الحجر الرملي النوبي تتغذى بشكل أساسي من المياه الجوفية القديمة، والتي تأثرت بعمليات التبخر، والمياه الجوفية العميقة الحارة، إضافة إلى عمليات الغسيل والإذابة.